

Inter-electron interactions and the RKKY potential between H adatoms in graphene

Pavel Buividovich,^{1,*} Dominik Smith,^{2,†} Maksim Ulybyshev,^{1,‡} and Lorenz von Smekal^{2,§}

¹*Institut für Theoretische Physik, Universität Regensburg, 93053 Regensburg, Germany*

²*Institut für Theoretische Physik, Justus-Liebig-Universität Gießen, 35392 Gießen, Germany*

(Dated: March 16, 2017)

We use first-principles Quantum Monte-Carlo simulations to study the Ruderman-Kittel-Kasuya-Yosida (RKKY) interaction between hydrogen adatoms attached to a graphene sheet. We find that the pairwise RKKY interactions at distances of a few lattice spacings are strongly affected by inter-electron interactions. We also analyse the stability of several regular adatom superlattices with respect to small displacements of a single adatom, distinguishing the cases of adatoms which populate either both or only one sublattice of the graphene lattice. We reveal the drastic difference in RKKY interactions in cases of anti-ferromagnetic (AFM) and charge density wave (CDW) orderings, which provides a qualitative explanation for the preferential attachment of adatoms to one sublattice, correlated with moiré structures in graphene on boron nitride.

PACS numbers: 73.22.Pr, 71.30.+h, 05.10.Ln

Introduction.—Functionalization of graphene with hydrogen adatoms or other admolecules which produce resonant scattering centers is currently a subject of intense research. First of all, it provides a way to create a band gap in graphene [1–3] with a possibility to tune it and even to return the material to the initial semi-metallic state [4]. Also the magnetic moments induced around hydrogen adatoms due to inter-electron interactions [3, 5, 6] play an important role in spin relaxation processes [7] and can be used to tune the magnetic properties of graphene.

The spatial distribution of adatoms plays a crucial role in the properties of hydrogenated graphene. For instance, magnetic moments of adatoms placed at different sublattices are coupled anti-ferromagnetically, while adatoms placed sufficiently close to each other on the same sublattice induce ferromagnetic ordering [3]. The stability (or instability) of these adatom configurations determines the magnetic properties of the functionalized material and might also explain the arrangement of hydrogen adatoms in regular superlattices observed in recent experiments [8, 9]. Especially important is the case of functionalized graphene on top of boron nitride [8], where hydrogen adatoms tend to occupy only one sublattice at special places in a moiré structure, forming islands of graphene.

The smallness of the pairwise elastic interaction of hydrogen adatoms in graphene, which does not exceed ~ 10 meV for distances larger than the inter-atomic spacing [10] and decays as r^{-3} at large distances [11], suggests that the Ruderman-Kittel-Kasuya-Yosida (RKKY) contribution from conduction electrons might dominate the inter-adatom interactions in graphene. So far, the RKKY potential between pairs of adatoms was studied analyti-

cally using some approximations to the fermionic Green's function in presence of resonant scatterers [12] and numerically within the non-interacting tight-binding model [13], and Density Functional Theory (DFT) [14, 15] which is known to under-estimate the effect of inter-electron interactions. For instance, it strongly underestimates the gap size in hydrogenated graphene [2], which is strongly enhanced by interactions even at moderate concentrations of adatoms, as suggested by the recent QMC study in Ref. [3].

In this paper we report on a first-principles Quantum Monte-Carlo (QMC) study of the RKKY interaction between hydrogen adatoms in graphene, consistently taking into account inter-electron interactions. We first consider pairwise interactions and demonstrate that for small distances between adatoms interaction effects dominate over the effects of finite temperature and finite hybridization terms. Then we consider the stability of adatom superlattices with respect to small shifts of a single adatom, finding the conditions for such a *dynamic* stability for various superlattices with adatoms occupying only one or equally both sublattices. It will be shown that the stability conditions are substantially different from those previously defined in Ref. [1]. The effect of antiferromagnetic (AFM) and charge density wave (CDW) ordering is also discussed, revealing an important feature of CDW order: the possibility to stabilize the superlattice configurations in which only one sublattice is occupied by hydrogen adatoms.

Numerical setup.—We describe electrons in the conduction band of graphene using the standard tight-binding Hamiltonian with nearest-neighbor hoppings on the hexagonal lattice and electrostatic inter-electron interactions:

$$\hat{H} = \sum_{\langle x,y \rangle, \sigma} -t_{xy} (\hat{a}_{y,\sigma}^\dagger \hat{a}_{x,\sigma} + h.c.) + \frac{1}{2} \sum_{x,y} V_{xy} \hat{q}_x \hat{q}_y, \quad (1)$$

where $\sum_{\langle x,y \rangle}$ and $\sum_{x,y}$ denote summations over all pairs $\langle x,y \rangle$ of nearest-neighbor sites and over all sites x, y of

*Electronic address: pavel.buividovich@physik.uni-regensburg.de

†Electronic address: dominik.smith@theo.physik.uni-giessen.de

‡Electronic address: maksim.ulybyshev@physik.uni-regensburg.de

§Electronic address: lorenz.smekal@theo.physik.uni-giessen.de

the graphene honeycomb lattice respectively. $\hat{a}_{x,\sigma}^\dagger$, $\hat{a}_{x,\sigma}$ are the creation/annihilation operators for electrons with spin $\sigma = \uparrow, \downarrow$ in carbon π -orbitals, t_{xy} are hopping amplitudes, $\hat{q}_x = -1 + \sum_{\sigma} \hat{a}_{x,\sigma}^\dagger \hat{a}_{x,\sigma}$ is the charge operator at site x and V_{xy} is the inter-electron interaction potential. Periodic spatial boundary conditions are imposed as in Refs. [16–18].

In this work we use two models of hydrogen adatoms on the graphene sheet. The first is the simple vacancy model describing hydrogen adatoms as missing lattice sites in the tight-binding Hamiltonian (1), so that hopping amplitudes t_{xy} are equal to zero for all neighbors y of the lattice sites x to which adatoms are attached. Away from adatoms, all hopping amplitudes are $t_{xy} = t = 2.7\text{ eV}$. Furthermore, we assume that each adatom has zero charge.

The second model is the full hybridization model [19], in which hybridization terms

$$\hat{H}_{hyb.} = \gamma \sum_{x \in \mathcal{H}, \sigma} (\hat{a}_{x,\sigma}^\dagger \hat{c}_{x,\sigma} + h.c.) + E_d \sum_{x \in \mathcal{H}, \sigma} \hat{c}_{x,\sigma}^\dagger \hat{c}_{x,\sigma}, \quad (2)$$

are added to the tight-binding Hamiltonian (1), where $\gamma = 2.0t$ is the hybridization parameter, $E_d = -0.06t$ is the electron energy for the adatom, $\sum_{x \in \mathcal{H}}$ denotes summation over all lattice sites with hydrogen adatoms and $\hat{c}_{x,\sigma}^\dagger$ are the creation operators for electrons on adatoms.

Since within the interacting tight-binding model the RKKY interaction is nothing but the fermionic Casimir potential, we calculate it as the free energy \mathcal{F}_{xy} of the electrons on the graphene lattice with adatoms at sites x and y [12, 20]. In absence of inter-electron interactions ($V_{xy} = 0$) we simply compute the corresponding single-particle energy levels ϵ_{xy} with adatoms numerically and obtain \mathcal{F}_{xy} up to an irrelevant constant F_0 from

$$\mathcal{F}_{xy} = -T \sum_{\epsilon_{xy}} \ln \left(1 + e^{-\epsilon_{xy}/T} \right) + F_0. \quad (3)$$

In order to treat inter-electron interactions, we use the Suzuki-Trotter decomposition followed by the Hubbard-Stratonovich transformation and represent the partition function $\mathcal{Z} = \exp(-\hat{H}/T)$ at temperature T as a path integral over Hubbard-Stratonovich fields $\phi_{x,\tau}$ in Euclidean time $\tau \in [0, T^{-1}]$ which is discretized, see Refs. [17, 18] (to maintain exact particle-hole and sublattice symmetries one can use an exponential transfer matrix for the fermions between adjacent time slices [21]):

$$\mathcal{Z} = \int \mathcal{D}\phi_{x,\tau} e^{-S[\phi_{x,\tau}]} |\det(M[\phi_{x,\tau}])|^2, \quad (4)$$

where $M = \partial_\tau - h_{xy} - i\phi_{x,\tau}\delta_{xy}$ is the fermionic operator and h_{xy} is the single-particle tight-binding Hamiltonian in (1). We sample the fields $\phi_{x,\tau}$ with the (manifestly positive) weight proportional to the integrand in (4) using the Hybrid Monte-Carlo algorithm. For the inter-electron interaction potential V_{xy} we use the potentials calculated with the constrained RPA method [22] for suspended graphene (see [3, 18] for details).

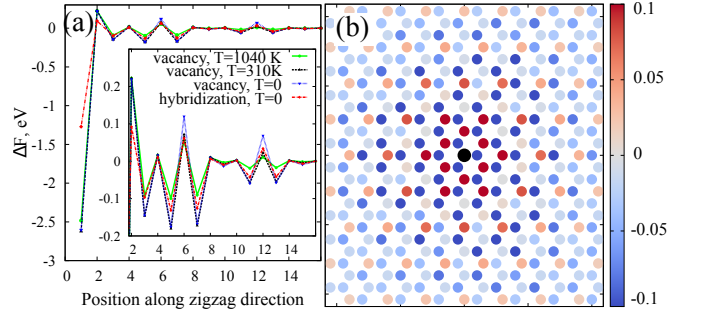


FIG. 1: Interaction of two adatoms calculated within the free tight-binding model on a lattice with 72×72 cells: (a) profile along zigzag direction (zoomed version in the inset); (b) 2D profile of RKKY potential for hybridization model (2) without inter-electron interactions at room temperature $T = 310\text{ K}$.

The free energy which enters the RKKY potential cannot be directly calculated in Hybrid Monte-Carlo simulations. To overcome this, we calculate the differences $\Delta\mathcal{F} = \mathcal{F}_{x+l,y} - \mathcal{F}_{x,y}$ between free energies for adatom positions which differ by a shift along one carbon-carbon lattice bond l . We represent this difference as an integral

$$\Delta\mathcal{F} = -T \int_0^1 d\alpha \partial_\alpha \log \mathcal{Z}_\alpha, \quad (5)$$

$$\mathcal{Z}_\alpha = \int \mathcal{D}\phi_{x,\tau} e^{-S[\phi_{x,\tau}]} |\det(M_\alpha[\phi_{x,\tau}])|^2, \quad (6)$$

where M_α linearly interpolates between fermionic operators with adatoms at positions x and y (at $\alpha = 0$) and $x+l$ and y (at $\alpha = 1$). Differentiating the path integral (6) for \mathcal{Z}_α by α , we express $\Delta\mathcal{F}$ as

$$\Delta\mathcal{F} = -2T \int_0^1 d\alpha \langle \text{Re Tr} (M_\alpha^{-1} \partial_\alpha M_\alpha) \rangle, \quad (7)$$

where the expectation value is calculated with the same path integral weight as in (6). The matrix $\partial_\alpha M_\alpha$ is very sparse, allowing for an efficient calculation of $\text{Tr} (M_\alpha^{-1} \partial_\alpha M_\alpha)$. The integral over α is calculated using the 6-point quadrature rule with six values of $\alpha \in [0, 1]$, including $\alpha = 0$ and $\alpha = 1$.

Pairwise interactions.—To study inter-adatom interactions in QMC simulations we use the simple vacancy model, since QMC has a fermion-sign problem for the hybridization model (2). For hydrogen adatoms the hybridization parameter $\gamma^2 \gg E_d t$ is sufficiently large, so that the corresponding sp^3 state of the carbon atom is effectively unavailable for p_z electrons [23] and the simple vacancy model is a good approximation to (2). In Fig. 1a we demonstrate that without inter-electron interactions the RKKY potentials are very similar for the hybridization model (2) and the vacancy model. In all cases, the pairwise interaction has well-known features: alternating signs for different sublattices [12] and the order-of-magnitude enhancement at some distances (clearly seen in Fig. 1b), at which the two adatoms induce midgap states with zero energy [13, 14].

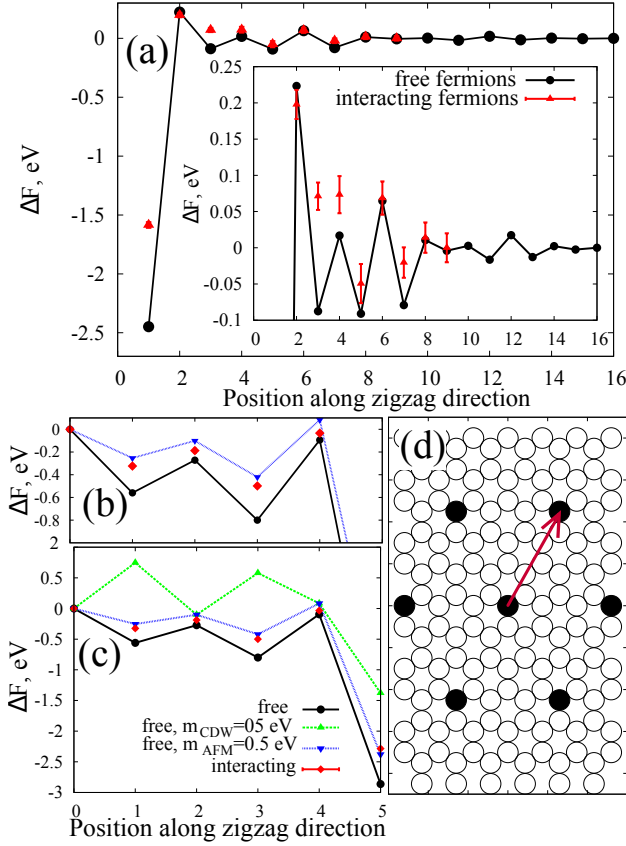


FIG. 2: RKKY interaction of two vacancies in the interacting tight-binding model (1) compared with the non-interacting case: (a) pairwise interaction (zoomed version in the inset); (b) and (c) free energy change of the superlattice system upon displacement of a single adatom (zoom-in and overview); and (d) superlattice structure with the zigzag profile used in figures (b) and (c) indicated by the red arrow (from simulations of a 24×24 lattice at $T = 0.09$ eV).

With reasonable computational resources, QMC simulations are limited to rather high temperatures in physical units ($T = 0.09$ eV = 1040 K here) which are still relatively small, however, compared to the typical energy scales of the interacting tight-binding model in Eq. (1). In Fig. 1 we demonstrate that at least in absence of inter-electron interactions such temperatures indeed do not affect the qualitative features of the pairwise RKKY interactions. This suggests that we may safely use the vacancy model for adatoms in QMC at $T = 0.09$ eV = $t/30$. We use lattices with 24×24 cells, for which finite-volume effects are smaller than statistical errors.

In Fig. 2a we illustrate the effect of inter-electron interactions on the RKKY potential along the zigzag direction, which is particularly strongly modified at distances of 3 and 4 C-C bonds. As a result, the local minimum at a distance of 3 bonds disappears and the potential barrier between widely separated adatoms and the global minimum corresponding to a dimer configuration becomes harder to penetrate.

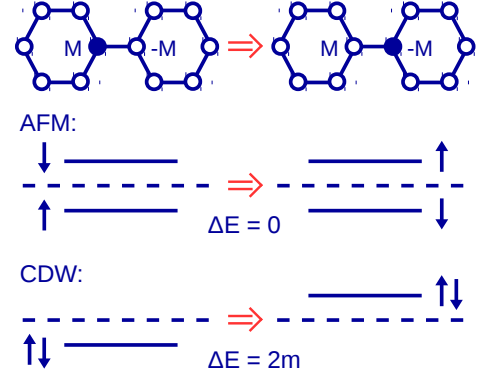


FIG. 3: Change of energy levels of Tamm states in presence of AFM and CDW mass terms: We illustrate the case in which one adatom moves from one sublattice to the other. The dashed line corresponds to the Fermi level.

Superlattices.—We now consider superlattices of regularly distributed hydrogen adatoms as examples of functionalization with a finite adatom concentration. To address superlattice stability, we first consider the variation of free energy accompanying the shift of a single adatom from its regular position along the zigzag direction, which is illustrated on Figs. 2b and 2c both for interacting and non-interacting tight-binding models. We chose the system with 5.56% coverage of hydrogen adatoms populating only one sublattice, as illustrated on Fig. 2d.

First we note that the overall scale of the RKKY interaction for superlattices is enhanced in comparison with pairwise interactions, so that the RKKY potential for a single adatom (with all other adatoms fixed) becomes comparable with the diffusion barriers $\Delta U \sim 0.3 \dots 1.0$ eV for hydrogen adatoms [24].

Surprisingly, for superlattices inter-electron interactions do not change the RKKY potential qualitatively, despite inducing a very large gap $\Delta\epsilon \sim 1$ eV in the midgap energy band [3]. To understand this observation, we recall that inter-electron interactions induce global anti-ferromagnetic (AFM) ordering for graphene with adatoms [3], with the effective mass term $\hat{M}_{AFM} = \pm m \sum_x (\hat{a}_{x\uparrow}^\dagger \hat{a}_{x\uparrow} - \hat{a}_{x\downarrow}^\dagger \hat{a}_{x\downarrow})$ which has alternating signs on different sublattices. We can estimate the change in the free energy upon the shift of a single adatom to the neighboring lattice site (and thus to another sublattice) assuming that 1) this change is determined mostly by Tamm states localized near this adatom and 2) the energy of this Tamm state can be estimated as the mass term at nearest-neighbour sites of the adatom (as the wavefunctions of the Tamm states are mostly localized on these sites). Since the AFM mass has different signs for different spin components, the states with different spins simply exchange their energies, and the overall sum of energies in (3) doesn't change in such a “mean field” approximation (see Fig. 3 for illustration).

The same argument applied to charge density wave

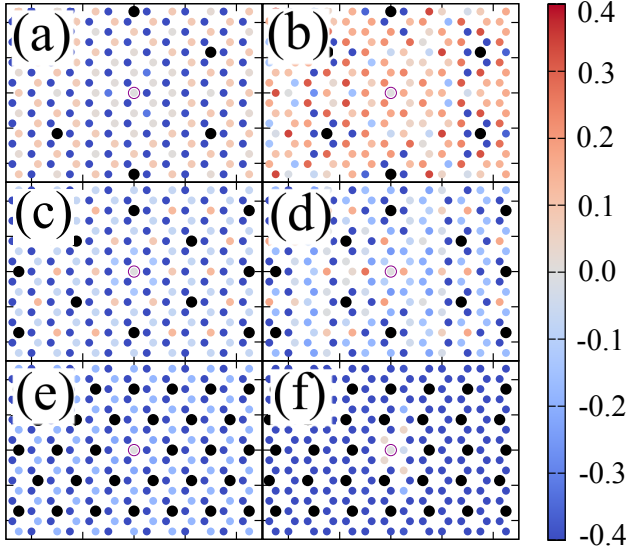


FIG. 4: Change of the free energy of superlattice systems upon the displacement of a single adatom. The fixed positions of other adatoms in the superlattices are marked with black dots. All plots correspond to half-filling. On the left: superlattices with only one sublattice populated by adatoms. On the right: superlattices of the the same densities of adatoms, but with equally populated sublattices.

(CDW) ordering leads to a completely different conclusion. Since in this case the mass term has the same sign for both spin components, the energies of two spin components no longer compensate each other, and the change of free energy upon adatom shift can be estimated as $2m$ (see Fig. 3). While we cannot check this scenario in QMC simulations, for which a CDW mass term leads to a sign problem [21], in Figs. 2b and 2c we illustrate the effects of both CDW and AFM mass terms on the RKKY potential for the hybridization model (2). We use $m = 0.5$ eV, which approximately corresponds to the AFM mass induced by inter-electron interactions. We indeed see that while the non-interacting result with AFM mass $m = 0.5$ eV almost coincides with the QMC result, the CDW mass term completely changes the RKKY potential and the locations of its minima.

The modification of the RKKY potential due to CDW ordering can be important for graphene grown on a boron-nitride substrate [25], which effectively induces a sizable CDW mass term in some regions of the moiré structure formed by the graphene and h-BN lattices. Because one expects the inter-electron interactions in presence of adatoms to further enhance this mass term, the overall effect can be very significant. Since for sufficiently large CDW mass the shift of a single adatom in the superlattice to the neighboring lattice site costs a large energy (see Fig. 2c), one concludes that adatoms should preferentially occupy only one of the two sublattices. And this is indeed also observed in experiments [8] where islands of graphene are seen in particular regions of a moiré structure.

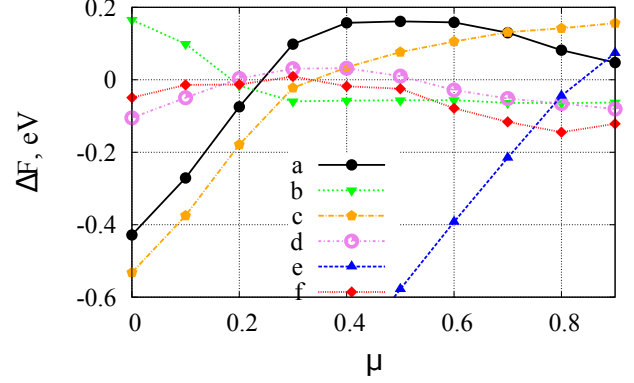


FIG. 5: The minimal change of the free energy accompanying the shift of a single adatom to the nearest neighbor position as a function of chemical potential. The alphabetic labels correspond to superlattices in Fig. 4. Negative values correspond to unstable superlattices.

In order to address the dynamic stability of superlattice configurations with only one or both sublattices populated by adatoms, we use the hybridization model (2) without inter-electron interactions. This seems fairly well justified because these interactions do not qualitatively change the RKKY potential and their quantitative effect can be mimicked by an explicit AFM mass quite well (see Fig. 2c). Previously it was shown [1] that unequally populated configurations are energetically favorable at half filling and at any positive doping. However, this observation does not in general imply the stability of superlattices with respect to adatom displacements. Indeed, as demonstrated in Fig. 4 we observe that the superlattices with adatoms on a single sublattice at half filling are dynamically unstable in all cases considered here.

In contrast, superlattices of adatoms which equally populate both sublattices are stable for low adatom concentration (see the structure in Fig. 4b). For higher adatom concentrations, all superlattices become unstable. This instability is likely to lead to the formation of dimers with a large binding energy.

Since a finite chemical potential can change the sublattice preferences of the pairwise RKKY interaction [13–15], the stability region of superlattices with only one sublattice occupied by adatoms might start from some finite positive chemical potential rather than at half-filling. In Fig. 5 we show the minimal change of the free energy among the three possible nearest-neighbor shifts as a function of the chemical potential μ for the same 6 adatom configurations as in Fig. 4. One can see that the single-sublattice superlattice with the lowest concentration of 3% adatoms (label “a”) does indeed become stable above $\mu \approx 0.25$ eV. At about the same value of μ the corresponding superlattice with equal population of adatoms on both sublattices on the other hand becomes unstable. The structures with equally populated sublattices are stable mainly near half-filling for low

concentrations of adatoms ($\leq 3\%$) or in some region of positive dopings for larger adatom concentrations. The larger the concentration, the smaller is the stability region. And vice versa for the single-sublattice configurations, the denser these adatom configurations get, the larger a chemical potential is needed to stabilize them.

Conclusions.—We have calculated the RKKY interaction potential between hydrogen adatoms on a graphene sheet, taking into account effects of electron-electron interactions in fully non-perturbative first-principles QMC simulations. In particular, we have studied both, pairwise potentials and free-energy differences with stability analyses for various configurations of finite adatom densities. For the pairwise RKKY potential we found that the inter-electron interactions tend to increase the potential barrier between widely separated adatom and dimer configurations which implies some suppression of dimer formation in the process of random deposition of adatoms on a graphene sheet.

For finite adatom concentrations, we have demonstrated that charge-density formation (CDW) and anti-ferromagnetic order (AFM) in the ground state, whether induced by substrates leading to staggered on-site potentials or dynamically by the inter-electron interactions,

have very different effects. While an AFM mass term does not qualitatively change the RKKY-type interaction, the effect of a CDW mass term can be much more significant and even influence the sublattice ordering of adatoms. This prediction could experimentally be further tested in hydrogen deposition on graphene attached to a boron-nitride substrate.

Our stability analyses of different hydrogen superlattices show that single-sublattice configurations of adatoms are unstable at half filling but can be stabilized by an appropriate amount of doping with chemical potentials $\mu > \mu_c$. The critical value μ_c thereby increases with increasing adatom concentrations. Superlattices with equally populated sublattices are stable near half-filling for low concentrations of adatoms. More densely populated superlattices are likely to be unstable towards dimer formation.

Acknowledgments.— This work was supported by the Deutsche Forschungsgemeinschaft (DFG), grants BU 2626/2-1 and SM 70/3-1. Calculations have been performed on GPU clusters at the Universities of Giessen and Regensburg. P.B. is supported by the S. Kowalevskaja award from the Alexander von Humboldt foundation.

-
- [1] D. A. Abanin, A. V. Shytov, and L. S. Levitov, Phys. Rev. Lett. **105**, 086802 (2010), [ArXiv:1004.3678](#).
 - [2] S. Putz, M. Gmitra, and J. Fabian, Phys. Rev. B **89**, 035437 (2014), [ArXiv:1309.1016](#).
 - [3] M. V. Ulybyshev and M. I. Katsnelson, Phys. Rev. Lett. **114**, 246801 (2015), [ArXiv:1502.01184](#).
 - [4] D. C. Elias, R. R. Nair, T. M. G. Mohiuddin, S. V. Morozov, P. Blake, M. P. Halsall, A. C. Ferrari, D. W. Boukhvalov, M. I. Katsnelson, A. K. Geim, et al., Science **323**, 610 (2009), [ArXiv:0810.4706](#).
 - [5] O. V. Yazyev and L. Helm, Phys. Rev. B **75**, 125408 (2007), [ArXiv:cond-mat/0610638](#).
 - [6] B. Wang and S. T. Pantelides, Phys. Rev. B **86**, 165438 (2012).
 - [7] W. Han, R. K. Kawakami, M. Gmitra, and J. Fabian, Nat. Nano **9**, 794 (2014), [ArXiv:1503.02743](#).
 - [8] R. Balog, B. Jorgensen, L. Nilsson, M. Andersen, E. Rienks, M. Bianchi, M. Fanetti, E. Laegsgaard, A. Baraldi, S. Lizzit, et al., Nat. Mater. **9**, 315 (2010).
 - [9] C. Lin, Y. Feng, Y. Xiao, M. Drr, X. Huang, X. Xu, R. Zhao, E. Wang, X.-Z. Li, and Z. Hu, Nano Lett. **15**, 903 (2015).
 - [10] P. S. Branicio, G. Vastola, M. H. Jhon, M. B. Sullivan, V. B. Shenoy, and D. J. Srolovitz, Phys. Rev. B **94**, 165420 (2016).
 - [11] P. Peyla and C. Misbah, Eur. Phys. J. B **33**, 233 (2003).
 - [12] A. V. Shytov, D. A. Abanin, and L. S. Levitov, Phys. Rev. Lett. **103**, 016806 (2009), [ArXiv:0812.4970](#).
 - [13] S. LeBohec, J. Talbot, and E. G. Mishchenko, Phys. Rev. B **89**, 045433 (2014), [ArXiv:1311.1796](#).
 - [14] D. Solenov, C. Junkermeier, T. L. Reinecke, and K. A. Velizhanin, Phys. Rev. Lett. **111**, 115502 (2013), [ArXiv:1301.5920](#).
 - [15] L. F. Huang, T. F. Cao, P. L. Gong, Z. Zeng, and C. Zhang, Phys. Rev. B **86**, 125433 (2012).
 - [16] P. V. Buividovich and M. I. Polikarpov, Phys. Rev. B **86**, 245117 (2012), [ArXiv:1206.0619](#).
 - [17] M. V. Ulybyshev, P. V. Buividovich, M. I. Katsnelson, and M. I. Polikarpov, Phys. Rev. Lett. **111**, 056801 (2013), [ArXiv:1304.3660](#).
 - [18] D. Smith and L. von Smekal, Phys. Rev. B **89**, 195429 (2014), [ArXiv:1403.3620](#).
 - [19] T. O. Wehling, S. Yuan, A. I. Lichtenstein, A. K. Geim, and M. I. Katsnelson, Phys. Rev. Lett. **105**, 056802 (2010), [ArXiv:1003.0609](#).
 - [20] M. Bordag, U. Mohideen, and V. Mostepanenko, Phys. Rep. **353**, 1 (2001), [ArXiv:quant-ph/0106045](#).
 - [21] P. Buividovich, D. Smith, M. Ulybyshev, and L. von Smekal, PoS LATTICE2016, 244 (2016), [ArXiv:1610.09855](#).
 - [22] T. O. Wehling, E. Şaşıoğlu, C. Friedrich, A. I. Lichtenstein, M. I. Katsnelson, and S. Blügel, Phys. Rev. Lett. **106**, 236805 (2011), [ArXiv:1101.4007](#).
 - [23] M. I. Katsnelson, Graphene: Carbon in Two Dimensions (Cambridge University Press, 2012).
 - [24] J. Talbot, S. LeBohec, and E. G. Mishchenko, Phys. Rev. B **93**, 115402 (2016), [ArXiv:1506.03422](#).
 - [25] G. Giovannetti, P. A. Khomyakov, G. Brocks, P. J. Kelly, and J. van den Brink, Phys. Rev. B **76**, 073103 (2007), [ArXiv:0704.1994](#).